Short Papers

Improved Error-Correction Technique for Large-Signal Load-Pull Measurements

ITAY HECHT

Abstract—**This article presents an improved vector error-corrected calibration technique for the well-known system used for large-signal characterization of oscillator and power amplifier transistors. The calibration procedure is very similar to conventional automatic network analyzer calibration procedures, and all its measurements, except for one power measurement, are performed by the system itself. Therefore, reflection coefficient and power level measurement accuracies of the system at both the input and output ports of the DUT are excellent, and are of the same order of magnitude as those of the automatic network analyzer.**

I. Introduction

Load-pull measurements are commonly used for the large-signal characterization of active devices used in microwave power amplifiers and oscillators. The advantages of this method are described in the literature [1]–[7]. The importance of accurate, error-corrected load-pull measurements is explained in [7], and a vector error-correction technique is described.

In general, prior to performing any measurements, the parameters of the error-correction model must be determined by some calibration procedure. This paper proposes a new calibration technique which is easier to use and yields more accurate output-port measurements than the one described in [7]. The measurement is performed by a vector network analyzer, such as the HP 8510, controlled and automated by a personal computer.

II. Measurement Setup

A block schematic of the load-pull measurement setup is shown in Fig. 1. The system is fed from a high-power microwave source, and the power level at the input of the DUT is controlled by a variable attenuator and by computer controlling the signal generator output level. Transmitted and reflected power waves at the input and output ports of the DUT are monitored by the network analyzer, using dual directional couplers. The network analyzer measures not only the large-signal reflection coefficients but also the power levels. A microwave power meter is used for calibrating the absolute power level reading of the network analyzer.

The load impedance is controlled manually using an output tuner (in this case a passive tuner, the Maury Microwave 2640D). The computer controls the calibration and measurement process via the GP-IB. It computes the error-correction parameters and displays the error-corrected load-contour map on a Smith chart.

III. Error Correction

The objective of the load-pull measurement is to provide large-signal error-corrected values for the reflection coefficients and signal power levels at the reference planes of the ports of the DUT. The transmitted and reflected power waves are shown in Fig. 2. The input reflection coefficient is $\Gamma_{in} = b_1/a_1$, the load reflection coefficient is $\Gamma_L = b_2/a_2$, and the input and output power levels are $P_{in} = |a_1|^2 - |b_1|^2 = |a_1|^2 \cdot (1 - |\Gamma_{in}|^2)$ and $P_{out} = |b_2|^2 - |a_2|^2 = |b_2|^2 \cdot (1 - |\Gamma_L|^2)$ respectively.

A. Flowgraph Model

Signal flowgraph modeling is a common way of presenting the power waves and the error-causing signals [8], [9]. A signal flowgraph that includes all predictable error sources is shown in Fig. 3. This is a redundant flowgraph in the sense that a branch in the graph sometimes sums the effect of more than one error source. The flowgraph presentation assumes that the network analyzer and the power meter are linear; hence their reflection coefficients are constant and independent of the signal power level. The model is presented in a different form from the model in [7], but is basically the same.

The input and output networks are shown in Fig. 3(a) and (b), respectively, where a_1' is the signal incident on the DUT, $\Gamma_1' = b_1'/a_1'$ and $\Gamma_2' = a_2'/b_2'$ are the uncorrected reflection coefficients measured by the network analyzer, $|P_1|^2$ and $|P_2|^2$ are the uncorrected power levels read by th network analyzer (or, alternatively, by power meters), E_{D_1}, E_{D_2}, and E_{D_2}' are directivity errors, E_{DR} is the reverse directivity error, E_{R_1}, E_{R_2}, and E_{R_2}' are frequency tracking errors, E_{S_1} and E_{S_2} are output reflection coefficients of the dual directional couplers and Γ_T is the input reflection coefficient of the tuner.

The error-corrected reflection coefficients and power levels are calculated directly from the flowgraphs in Fig. 3:

$$\Gamma_{in} = \frac{\Gamma_1' - E_{D_1}}{E_{S_1} \cdot (\Gamma_1' - E_{D_1}) + E_{R_1}} \tag{1}$$

$$P_{in} = \frac{|P_1|^2}{|E_{P_1}|^2} \cdot \frac{1 - |\Gamma_{in}|^2}{|1 - \Gamma_{in} \cdot E_{S_1}|^2} \tag{2}$$

$$\Gamma_2 = \frac{a_2}{b_2} = E_{D_2} + \frac{\Gamma_2' - E_{D_2}'}{E_{R_2}'/E_{R_2} - E_{DR}/E_{R_2} \cdot (\Gamma_2' - E_{D_2}')} \tag{3}$$

$$P_{out} = \frac{|P_2|^2}{|E_{P_2}|^2} \cdot \frac{|\Gamma_2' - E_{D_2}'|^2 \cdot (1 - |\Gamma_L|^2)}{|E_{R_2}'/E_{R_2}|^2 \cdot |\Gamma_L - E_{D_2}|^2}. \tag{4}$$

B. Calibration — Input Port

The calibration for the Γ_{in} measurement is made according to HP's standard automatic network analyzer techniques [9], where the DUT is replaced by three calibration standards. In this case a sliding load (measured at three or more positions of the load), an open circuit, and a short circuit are used as calibration standards, but other choices (one of which is mentioned in [7]) are possible, as mentioned in [10]. The measurement of the three calibration standards provides all the three error terms in (1) and (2). The $|E_{P_1}|^2$ term is obtained by connecting a power meter in place of the DUT. Γ_{in} of the power meter is measured by the ANA and corrected by (1), then $|E_{P_1}|^2$ is calculated from (2).

Manuscript received March 3, 1987; revised July 7, 1987
The author is with the General Microwave Israel Corporation, P.O. Box 8444, Jerusalem 91083, Israel
IEEE Log Number 8716916.

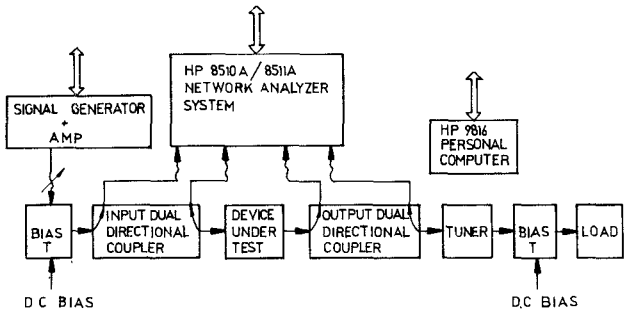

Fig. 1. Block schematic of the load-pull setup.

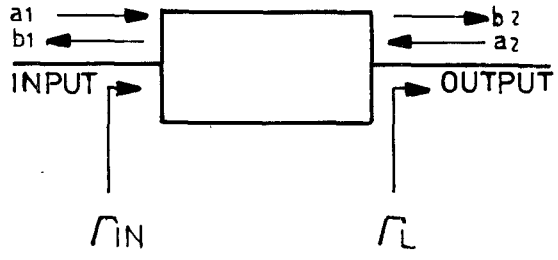

Fig 2. Power waves at the reference planes of the DUT.

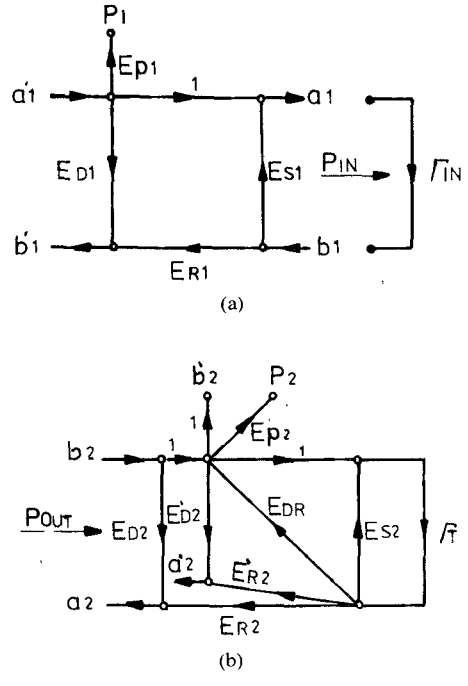

Fig. 3. Signal flowgraph error model (a) Input port. (b) Output port.

C. Calibration — Output Port

The output port calibration technique comprises the innovative portion of this paper. The calibration is obtained by using the already calibrated input port to calibrate the output port. The two dual directional couplers are through-connected, so that $a_1 = b_2$, $b_1 = a_2$, and $\Gamma_{in} = \Gamma_L$, and the tuner is replaced with the calibration standards. Just as in the input port case, four calibration measurements are taken.

First, a sliding load (HP recommends using fixed loads at frequencies up to 2 GHz for 7-mm connectors and up to 4 GHz for 3.5-mm connectors and sliding loads for higher frequencies, due to the degradation of the matching of the fixed loads; incidentally, this applies also to the calibration of the input port)

FREQ IS 4.E+9

$\lvert\Gamma_{IN}\rvert$	$\angle\Gamma_{IN}$ [Deg]	$\frac{\lvert\Gamma_L - \Gamma_{IN}\rvert}{\lvert\Gamma_{IN}\rvert}$ [dB]	$\frac{P_{OUT}}{P_{IN}}$ [dB]
.1	17	-57.5	.0037
.2	67	-59.9	.0046
.3	98	-59	.0055
.4	153	-57.1	.009
.51	-148	-58.1	.0045
.59	-88	-55.4	.0023
.72	-15	-55.7	.005
.75	-152	-59.5	.0094
.68	79	-61	.011

Fig. 4. Accuracy check.

is connected, and E_{D_2} and E'_{D_2} of (3) are calculated (Γ_L is measured and corrected by the input network error correction). Then a short circuit and an open circuit are used in order to calculate E'_{R_2}/E_{R_2} and E_{DR}/E_{R_2} by (3). Two unknown loads can also be used in this case, instead of open and short circuits, but their impedances must differ from one another. The $|E_{P_2}|^2$ term is calculated through (4), using the calibration standard that was used for the previous measurement, i.e., the open circuit. Γ_L and P_{out} are measured and corrected by the input network, so a power meter is not required.

IV. Accuracy Check

The accuracy of the computer-corrected input port measurement is inherently the same as that of the automatic network analyzer, as it is calibrated in the same way as the ANA is calibrated.

The output port computer-corrected measurement is expected to yield about the same accuracy because it is calibrated in a very similar manner. This accuracy was checked by comparing Γ_L and P_{out} to Γ_{in} and P_{in}, for different tuner positions, when the input and output ports were through-connected (as in the output port calibration). This comparison yielded reflection coefficient vector errors of less than -50 dB and power differences of less than ± 0.02 dB. An example of an accuracy check at 4 GHz with 7-mm connectors is shown in Fig. 4. It seems that this accuracy is about the best that can be achieved by the ANA and it is also better than the ± 0.15-dB accuracy reported in [7]. The reason for the reduced accuracy of [7] is probably the use of several approximations in the output calibration process.

V. Conclusions

A load-pull measurement error correction technique has been described. This technique introduces a new calibration method for the output port error-correction model, and yields excellent measurement accuracy for both the input and output port reflection coefficients and power levels (equivalent output port measurement accuracy has not been reported until now).

The measurement is performed by an ANA (automatic network analyzer) and utilizes a full-term vector error-correction model. The error-correction calibration procedure is simple and requires a minimum number of connections, with most of the calibration measurements being performed by the measurement system.

The technique can be used for both 2-port (amplifier) and output port (oscillator) measurements. However, even output port measurements require a 2-port calibration.

ACKNOWLEDGMENT

The author wishes to thank Y. Adelman, Supervisor of the project, for his time spent reviewing this paper and his associated comments, and R. Engelberg, his colleague, for also reviewing this paper.

REFERENCES

[1] J M. Cusack *et al*, "Automatic load contour mapping for microwave power transistors," *IEEE Trans. Microwave Theory Tech*, vol. MTT-22, pp. 1146–1152, Dec. 1974.
[2] Y. Takayama, "A new load-pull characterization method for microwave power transistors," in *Dig. IEEE 1976 Int Microwave Symp.*, pp. 218–220.
[3] R. B. Stancliff and D D Poulin, "Harmonic load pull," in *Dig. IEEE 1979 Int. Microwave Symp.*, pp. 185–187.
[4] H. Abe and Y. Aono, "11 GHz GaAs power MESFET load-pull measurements utilizing a new method for determining tuner y parameters," *IEEE Trans. Microwave Theory Tech.*, vol. MTT-27, pp 394–399, May 1979.
[5] D Poulin, "Load-pull measurement help you meet your match," *Microwaves*, pp 61–65, Nov. 1980.
[6] G P Bava *et al.*, "Active load techniques for load-pull characterization at microwave frequencies," *Electron. Lett*, vol. 18, pp. 178–180, 1982
[7] R. S. Tucker and P. D. Bradley, "Computer-aided error correction of large-signal load-pull measurements," *IEEE Trans Microwave Theory Tech*, vol. MTT-32, pp 296–300, Mar. 1984.
[8] N. Kuhn, "Simplified signal-flow-graph analysis," *Microwave J.*, pp. 59–66, Nov. 1963.
[9] "Automating the HP8410B microwave network analyzer," HP Appl. Note 221A, June 1980
[10] E. F. Da Silva and M. K. McPhun, "Calibration techniques for one-port measurements," *Microwave J.*, pp. 97–100, June 1978.

Latching Ferrite Quadrupole-Field Devices

YANSHENG XU

Abstract—**In this paper a brief survey of research and development on latching ferrite quadrupole-field devices in China is presented. Initially, theoretical analyses and some general rules for these kinds of devices are given. Some practical construction techniques and experimental results are also presented. Finally, many practical devices are described (e.g. reciprocal phase shifters with fast switching polarizations, reciprocal phase shifters with transverse magnetization, duplex phase shifters). In general, latching ferrite quadrupole-field devices have many advantages, among them simplicity, ruggedness, and rapid switching.**

I. INTRODUCTION

Dual-mode ferrite devices have found widespread applications as polarizers, phase shifters, etc. In recent years the latching version of one of the most popular dual-mode devices—quadrupole-field ferrite devices—has been used in China [1], and theoretical and experimental work on them has been performed. Many new devices are constructed or are under development.

Manuscript received February 18, 1987; revised June 29, 1987
The author is with the Beijing Institute of Radio Measurement, P.O Box 3923, Beijing, China.
IEEE Log Number 8716595.

II. THEORY

Dual-mode ferrite devices are constructed in square or circular waveguides, and are usually analyzed by the coupled wave theory suggested by Schelkunoff more than 30 years ago [2]. First, we calculate the tensor permeability of ferrite, magnetized in an arbitrary direction. Generally speaking, the direction of magnetization changes from point to point, and at any point in space we use Cartesian coordinates (x, y, z) and allow the z axis to coincide with the direction of magnetization at this point. Then, we have

$$\begin{aligned} B_x &= \mu H_x - jkH_y \\ B_y &= jkH_x + \mu H_y \\ B_z &= \mu_z H_z . \end{aligned} \tag{1}$$

It is necessary to point out that the coordinates x, y, z in (1) change everywhere in space, and for simplicity we may write (1) as

$$\vec{B} = \mu\vec{H} + (\mu_z - \mu)(\vec{\gamma}\cdot\vec{H})\vec{\gamma} + jk\vec{\gamma}\times\vec{H} \tag{2}$$

where $\vec{\gamma}$ is the unit vector along the z axis (i.e., direction of magnetization at this point). In the calculation of dual-mode ferrite devices, the unit vector $\vec{\gamma}$ should be represented as the superposition of unit vectors of arbitrary orthogonal coordinates (u, v, w), used in our boundary value problem of electromagnetic theory:

$$\vec{\gamma} = \gamma_u\vec{u} + \gamma_v\vec{v} + \gamma_w\vec{w}$$

where $\vec{u}, \vec{v}, \vec{w}$ are unit vectors in the directions (u, v, w), and $\gamma_u, \gamma_v, \gamma_w$ are the projections of $\vec{\gamma}$ in the directions (u, v, w) respectively, and are functions of (u, v, w). From (2) we obtain the following tensor permeability in the coordinates (u, v, w):

$$\|\mu\| = \begin{bmatrix} \mu & -jk\gamma_w & jk\gamma_v \\ jk\gamma_w & \mu & -jk\gamma_u \\ -jk\gamma_v & jk\gamma_u & \mu \end{bmatrix} + (\mu_z - \mu)\begin{bmatrix} \gamma_u^2 & \gamma_u\gamma_v & \gamma_u\gamma_w \\ \gamma_u\gamma_v & \gamma_v^2 & \gamma_v\gamma_w \\ \gamma_u\gamma_w & \gamma_v\gamma_w & \gamma_w^2 \end{bmatrix}. \tag{3}$$

For weakly magnetized ferrites $\mu_z \approx \mu$ and

$$\|\mu\| = \begin{bmatrix} \mu & -jk\gamma_w & jk\gamma_v \\ jk\gamma_w & \mu & -jk\gamma_u \\ -jk\gamma_v & jk\gamma_u & \mu \end{bmatrix}. \tag{4}$$

Although (3) and (4) have already been obtained in other forms by coordinate transformations in the literature [3], this equation is very convenient and useful in calculating dual-mode ferrite devices, as shown in the following.

From Schelkunoff [2], we may expand the electromagnetic fields in waveguides containing transversely magnetized ferrites as the superposition of normal modes of electromagnetic waves in the empty waveguide (in the following, coordinate z coincides